Human Molecular Genetics, 2007, Vol. 16, No. 16 ***1993–2003***
doi:10.1093/hmg/ddm147
Advance Access published on June 21, 2007

MPP1 links the Usher protein network and the Crumbs protein complex in the retina

Ilse Gosens[1,4], Erwin van Wijk[1,2,4], Ferry F.J. Kersten[1,2,4], Elmar Krieger[3,4], Bert van der Zwaag[5], Tina Märker[6], Stef J.F. Letteboer[1], Simone Dusseljee[1], Theo Peters[2], Henk A. Spierenburg[5], Ingrid M. Punte[1], Uwe Wolfrum[6], Frans P.M. Cremers[1,4], Hannie Kremer[2,†] and Ronald Roepman[1,4,*†]

[1]Department of Human Genetics, [2]Department of Otorhinolaryngology, [3]Center for Molecular and Biomolecular Informatics, [4]Nijmegen Centre for Molecular Life Sciences, Radboud University Nijmegen Medical Centre, Geert Grooteplein Zuid 10, PO Box 9101, 6500 HB, Nijmegen, The Netherlands, [5]Department of Pharmacology and Anatomy, Rudolf Magnus Institute of Neuroscience, University Medical Centre Utrecht, Utrecht, The Netherlands and [6]Department of Cell and Matrix Biology, Institute of Zoology, Johannes Gutenberg University of Mainz, Mainz, Germany

Received March 15, 2007; Revised and Accepted June 10, 2007

The highly ordered distribution of neurons is an essential feature of a functional mammalian retina. Disruptions in the apico-basal polarity complexes at the outer limiting membrane (OLM) of the retina are associated with retinal patterning defects in vertebrates. We have analyzed the binding repertoire of MPP5/Pals1, a key member of the apico-basal Crumbs polarity complex, that has functionally conserved counterparts in zebrafish (nagie oko) and *Drosophila* (Stardust). We show that MPP5 interacts with its MAGUK family member MPP1/p55 at the OLM. Mechanistically, this interaction involves heterodimerization of both MAGUK modules in a directional fashion. MPP1 expression in the retina throughout development resembles the expression of whirlin, a multi-PDZ scaffold protein and an important organizer in the Usher protein network. We demonstrate that both proteins interact strongly by both a classical PDZ domain-to-PDZ binding motif (PBM) mechanism, and a mechanism involving internal epitopes. MPP1 and whirlin colocalize in the retina at the OLM, at the outer synaptic layer and at the basal bodies and the ciliary axoneme. In view of the known roles of the Crumbs and Usher protein networks, our findings suggest a novel link of the core developmental processes of actin polymerization and establishment/maintenance of apico-basal cell polarity through MPP1. These processes, essential in neural development and patterning of the retina, may be disrupted in eye disorders that are associated with defects in these protein networks.

INTRODUCTION

The specialized layered structure of the neural retina is a fundamental, conserved feature that is essential for the correct perception of detailed visual images. In addition to the layered assembly of the different retinal cell types and their processes, cells are also distributed in a highly organized fashion within the plane of each cell layer. This retinal organization allows the different cell types and their processes to form a dense meshwork of cell-to-cell contacts, necessary to transfer, process and adapt to intercellular signaling information. Aside from the fact that the differentiated layers of the retina consist of seven major cell classes, studies in zebrafish have shown that all retinal cells originate from a single sheet of morphologically uniform neuroepithelium (1). In fully stratified adult retinae, the apical cell junctions of this epithelium are retained, forming a layer of cell–cell adhesive contacts between photoreceptors and Müller glia cells: the outer limiting membrane (OLM). During development, retinal cell types migrate away from the neuroepithelium to

*To whom correspondence should be addressed. Tel: +31 24 3610487; Fax: +31 24 3668752; Email: r.roepman@antrg.umcn.nl
†The authors wish it to be known that, in their opinion, the last two authors should be regarded as joint senior authors of this paper.

form the inner retinal layers. Although little is known about the molecular cues guiding the positioning of neurons in the mammalian retina, the disturbed retinal patterning of the zebrafish *nok* (2), *ome* (3,4), *has* (3), *glo* (3,5) and *moe* (6) mutants indicates that the associated proteins, MPP5/Pals1 (2,7), Crb2a (8), aPKC (9), N-cadherin (10) and EPB41L5/YMO1, respectively (11,12), are crucial for retinal integrity. These proteins are all part of the apico-basal polarity complexes at tight junctions and adherens junctions of mammalian epithelial cells. In *Drosophila*, the asymmetric distribution of transmembrane protein Crumbs and its binding partner Stardust (*Drosophila* homologue of MPP5/nok), is instrumental for the generation and maintenance of cell polarity and for the regulation of epithelial junction assembly (13–15).

Mutations in human *Crumbs homologue 1* (*CRB1*) lead to inherited retinal degenerations such as Leber congenital amaurosis (LCA) and retinitis pigmentosa (RP) (16). The encoded polypeptide localizes apically to the OLM of the mammalian retina (17), where it interacts with MPP5 (18,19). At this location MPP5 organizes a protein scaffold that includes the MAGUK family members MPP3 (20) and MPP4 (19). In addition, MPP5 has also been found to interact with Lin-7 (21), PAR6 (22), PATJ (23), MUPP1 (18), Ezrin (24) and the neuronal GABA transporter GAT1 (25).

We here describe the identification of the specific interaction between MPP5 and MPP1, a.k.a. erythrocyte protein p55 and their colocalization at the OLM. In addition to Crumbs protein complex members, some Usher proteins, including whirlin/CIP98 have been identified at the OLM (26). Our results indicate that the multi-PDZ protein whirlin also binds to MPP1 at this subcellular site. In addition, whirlin-MPP1 colocalization was determined in the outer plexiform layer (OPL), containing the synaptic processes of the photoreceptors, and at the region of the photoreceptor cilium. Mutations in *whirlin* are implicated in isolated deafness (type DFNB31) (27) and in Usher syndrome (type USH2D) (28). In the inner ear, whirlin was found to be essential in stereocilia organization, and an important mediator of actin polymerization (27,29). Our current findings suggest a link of the core developmental processes of actin polymerization and generation or maintenance of cell polarity through MPP1 interaction with MPP5 and whirlin.

RESULTS

MPP5 specifically interacts with MPP1

Since MPP5 contains a number of protein–protein interaction domains (Fig. 1A), a scaffolding function was assigned to this protein. To identify interactors for the SH3 + HOOK domain of MPP5, we previously screened a human oligo-dT primed retinal cDNA library and isolated MPP4 as an interacting protein (19). As homology modeling suggested a potential heterodimerization of different MPP family members, we expanded the yeast two-hybrid screening using an optimized cell-to-cell mating protocol. Besides MPP4, we identified 13 prey clones expressing MPP1 (Fig. 1B), but no other clones for MPP family members. All MPP1 clones contained part of the SH3 domain, the HOOK domain and GUK domain. Unlike other MAGUK family members, MPP1 does not contain L27 domains. The $MPP1^{E\text{-}end}$ and $MPP1^{SH3+HOOK}$ constructs were used in yeast two-hybrid (Fig. 1C) as well as biochemical assays (Fig. 1D; Supplementary Material, Fig. S7) to pinpoint the interacting domains of MPP1 and MPP5 and determine their binding specificity. Yeast two-hybrid analysis of several MPP1 and MPP5 constructs showed that the interaction is directional (Fig. 1C); the $MPP1^{prey}$ containing the GUK domain interacts with the SH3 + HOOK domain of MPP5, but the SH3 + HOOK domain of MPP1 lacks binding affinity for the GUK domain in $MPP5^{HOOK\text{-}end}$. In addition, the SH3 + HOOK domain of MPP1 can bind the $MPP1^{E\text{-}end}$ protein that contains the GUK domain. This indicates that, similar to other MPP and MAGUK proteins, the SH3 and GUK molecules are involved in intramolecular binding in the same fashion as its intermolecular binding with MPP5. This intramolecular binding may prevent homodimerization *in vitro*, as we could not detect interaction of the full length MPP1 proteins in the yeast two-hybrid assay. GST-pull down analysis confirmed the interaction between the SH3 + HOOK domain of MPP5 and the C-terminus of MPP1 (Fig. 1D; Supplementary Material, Fig. S7).

Analysis of the MPP1–MPP5 interaction by molecular modeling

In our initial work on the MPP4–MPP5 interaction, molecular modeling predicted a high binding affinity due to several salt-bridges (19). Here we repeated the analysis not only for MPP1–MPP5, but also for all six homo- and heterodimers that can be formed by MPP1, MPP4 and MPP5. *In silico* binding energies were calculated as described previously (19) and are listed in Table 1. The predicted binding energy of the MPP4 homodimer was the highest, followed by MPP4–MPP5, while dimers involving MPP1 are ranked last. Visual inspection shows that this is mainly due to a smaller contact interface with fewer salt-bridges. Nevertheless, homology modeling of the MAGUK modules supports MPP1–MPP5 heterodimer formation (Fig. 1E), and is predicted to reach an affinity close to MPP5–MPP5 (Table 1).

MPP1 binds MPP5 at the outer limiting membrane of the retina

Expression analysis by semi-quantitative RT–PCR on a panel of RNAs from several human tissues showed that *MPP1* is ubiquitously expressed as other *MPP* family members, except MPP4, which is mainly found in the retina (Supplementary Material, Fig. S8). We used RNA *in situ* hybridization on mouse cryosections to monitor the cellular levels of *MPP1* transcripts, and detected a distinct signal in the eye from E14.5 onwards. Intense staining was present in the liver and primitive gut, whereas the umbilical vein, the ventricular layer of the CNS and upper/lower jaw region showed lower signal intensity (Fig. 2A). At E14.5 (Fig. 2B) and E16.5, expression in the liver and stomach was maintained. In addition, expression was present in bone structures (e.g. zygomatic bone, lower jawbone), cranial nerve ganglia [e.g. trigeminal (V) ganglion] and cochlea (Fig. 2D). When viewed at higher magnification, the expression of *MPP1* in

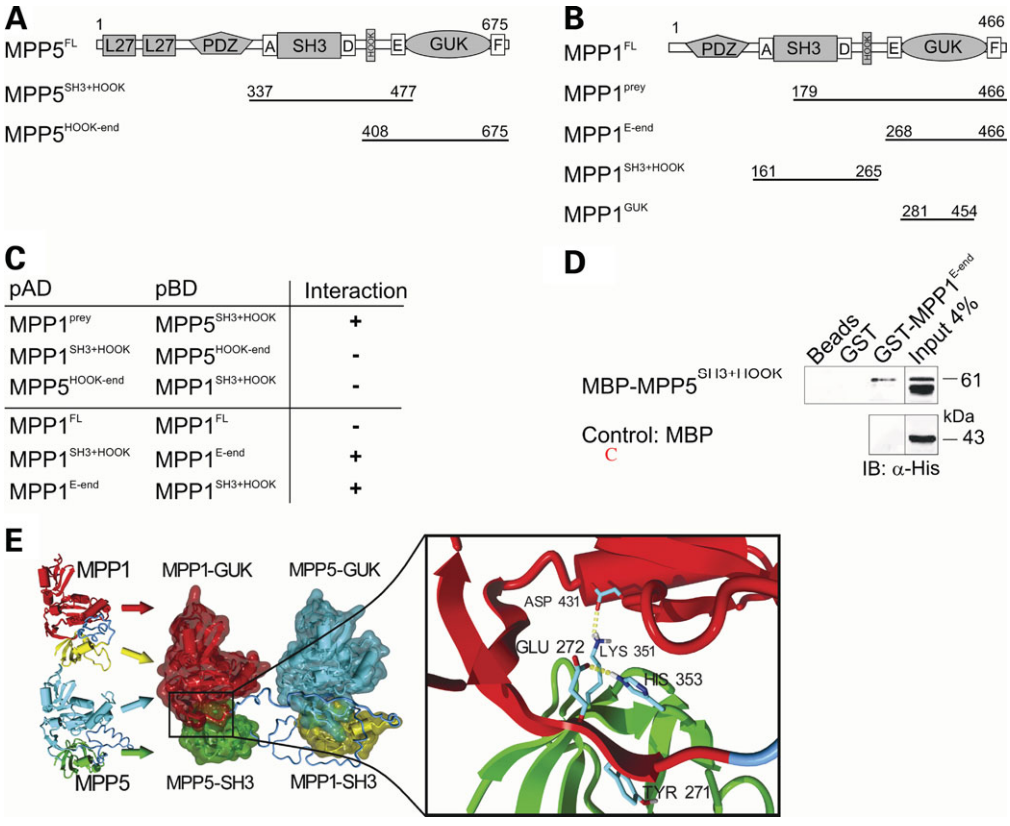

Figure 1. MPP5 binds to MPP1 by a GUK/SH3 domain swap. (**A**) Schematic representation of the overall domain composition of MAGUK protein MPP5. Two L27 domains and the MAGUK module containing a PDZ, SH3 and GUK domain are present. A HOOK domain is found between the SH3 and GUK domain. Strands A and D flanking the SH3 domain and E and F flanking the GUK domain were identified according to homology with PSD-95. $MPP5^{SH3+HOOK}$ was used as bait. The $MPP5^{HOOK\text{-}end}$ construct is used in a yeast two-hybrid assay to determine the specificity of the interaction between MPP1 and MPP5. (**B**) Identical MPP1 preys were found and $MPP1^{E\text{-}end}$, $MPP1^{SH3+HOOK}$, $MPP1^{GUK}$ and $MPP1^{FL}$ constructs were made. (**C**) The $MPP1^{prey}$ interacts with the $MPP5^{SH3+HOOK}$, but $MPP1^{SH3+HOOK}$ does not bind to $MPP5^{HOOK\text{-}end}$. Full-length MPP1 proteins do not bind to each other, whereas selected parts of the MAGUK modules do. (**D**) GST-$MPP1^{E\text{-}end}$ pulled down $MPP5^{SH3+HOOK}$. Beads alone or GST did not interact with MPP5, while MPP1 did not bind the MBP tag in the control experiment, showing that this interaction is specific. (**E**) Homology modeling of the MAGUK modules of MPP1 and MPP5. The interacting GUK and SH3 domains of MPP1 (red and yellow, respectively) and MPP5 (cyan and green) separate and form a heterodimer consisting of two mixed GUK/SH3 complexes. The domain linker regions in MPP1 and MPP5 (shown in blue) are both long enough to support this rearrangement. The proposed mechanism of the MPP1–GUK/MPP5–SH3 (red, green) interaction is shown as a close-up: Lys 351 and His 353 in MPP5-SH3 interact with Asp 431 and Glu 272 in MPP1-GUK via a salt-bridge and a hydrogen bond, respectively. In addition, the GUK domain places Tyr 271 in the hydrophobic core of the SH3 domain, a strong but unspecific interaction found in all heterodimers.

Table 1. Estimated *in silico* binding energies for the six different dimers of MPP1, 4 and 5, sorted from highest to lowest affinity

Complex	Energy (kcal/mol)
MPP4–MPP4	378
MPP4–MPP5	323
MPP5–MPP5	294
MPP1–MPP5	283
MPP1–MPP4	266
MPP1–MPP1	250

Each binding energy is the sum of two GUK–SH3 interactions.

the eye could be ascribed to the neuroblastic layer (Fig. 2F), the same cell layer in which the *whirlin* transcript was found to be expressed (26). At E16.5 and E18.5 a slightly higher intensity of staining in the neuroblastic layer was seen (Fig. 2G and H). At E16.5, strong staining in the upper part of the gut was maintained and with the onset of ossification, expression was seen in all bone structures of the body (e.g. femur, Fig. 2E). At P7 and P90, *MPP1* expression in the eye was identified in the ganglion cell layer, the inner nuclear layer (INL) and photoreceptor cell layer (Fig. 2I and J).

The subcellular localization of MPP1 in the retina was analyzed using polyclonal antibodies against MPP1 in cryosections of the rat retina. We detected MPP1 expression in the OPL, the OLM, the inner segments (IS), around the nuclei of the outer nuclear layer (ONL) and at the connecting cilium (CC) region that separates the inner and the outer segments, with both anti-MPP1 rabbit and mouse sera. In addition, MPP1 was detected in the retinal pigment epithelium (RPE) (Fig. 3A1). No staining in the inner nuclear layer, inner plexiform layer and ganglion cell layer was found (data not shown), although the MPP1 transcript was detected in the

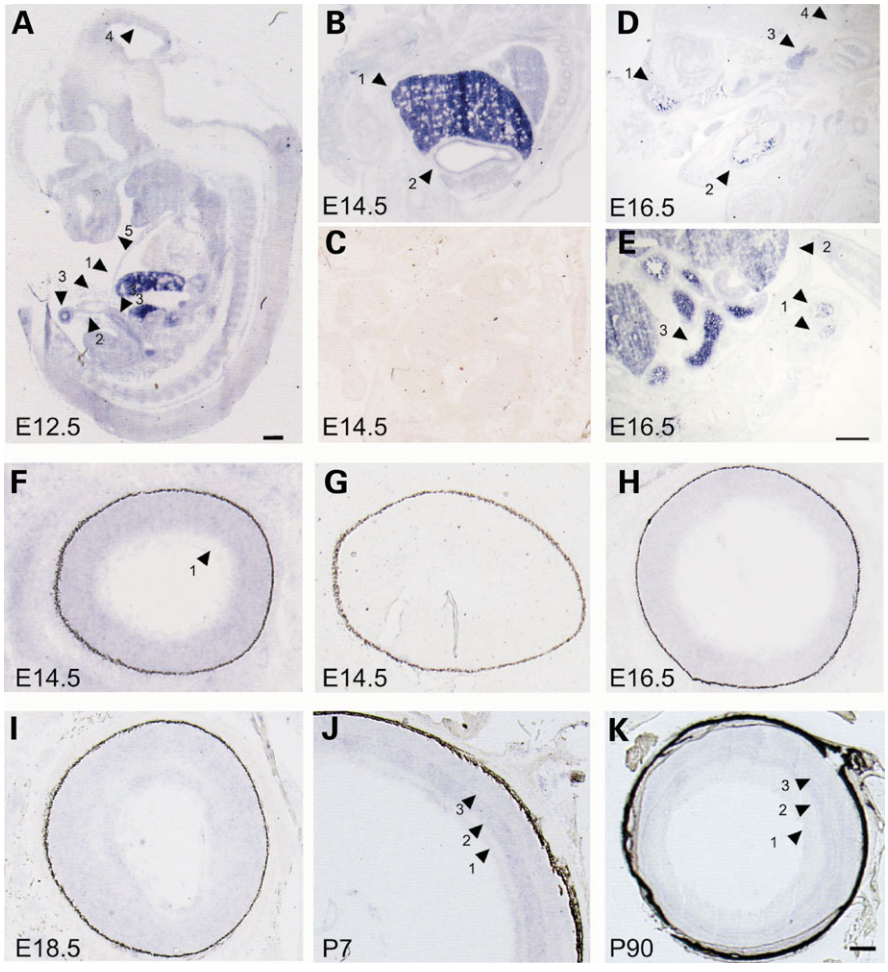

Figure 2. *MPP1* expression analysis by RNA *in situ* hybridization on embryonic and adult mouse tissues. In sagittal whole embryo cryosections low levels of expression were seen throughout the embryo. (**A**) *MPP1* expression at E12.5 in (1) liver; (2) umbilical vein; (3) primitive gut; (4) neuroepithelium; and (5) upper jaw region. Scalebar is 300 μm. (**B**) At E14.5, expression was maintained in (1) the liver; and (2) stomach. (**C**) Hybridization with a *MPP1* sense probe did not show tissue labeling. (**D**) At E16.5, the (1) zygomatic bone; (2) lower jawbone; (3) trigeminal (V) ganglion; and (4) cochlea showed expression of *MPP1*. (**E**) A strong signal was also observed in (1) femur; (2) liver; and (3) small intestine at this stage. Scalebar is 20 μm. (**F**) In the eye, a slightly higher signal intensity compared with surrounding tissues was observed in the inner neuroblastic layer. (**G**) No staining was observed in the eye after sense probe hybridization. (**H**) At E16.5 and (**I**) E18.5, expression was maintained in the neuroblastic layer and appeared in the developing photoreceptor layer. (**J**) At P7 and (**K**) P90, expression in (1) ganglion cells; (2) inner nuclear layer (INL); and (3) photoreceptor cell layer was seen. Scalebar is 20 μm.

latter. Co-staining with anti-β-catenin, a marker for the OLM and OPL, confirmed the presence of MPP1 at these locations (Fig. 3A2 and A3 and C2). Co-staining with CC marker acetylated tubulin revealed some overlap, but most of the MPP1 signal is detected just below the axoneme of the CC (Fig. 3B). Costaining of retinal sections with antibodies against MPP1 and MPP5 confirmed their colocalization at the OLM in the rat (Fig. 3C) as well as in the mouse retina (data not shown).

Immunoprecipitations from retinal lysates were performed to detect a physical interaction between MPP1 and MPP5. Anti-MPP5 antibody precipitated both MPP5 (75 kDa) as well as MPP1 (55 kDa) from bovine and mouse retinas (Fig. 3D, left panels and data not shown). The reciprocal immunoprecipitation experiment using anti-MPP1 coprecipitated MPP5, confirming their presence in the same protein complex (Fig. 3D, right panel).

MPP1 binds whirlin at multiple subcellular locations in the retina

Although a whirlin–MPP1 interaction has previously been described (30), the mechanism of interaction was not analyzed in detail. We used different fragments of the long isoform of whirlin (Fig. 4A) to determine the epitopes interacting with the C-terminus of MPP1 that is homologous to the C-terminus of CASK (Fig. 4B), another known interactor of whirlin (30). Using yeast two-hybrid analysis, we could determine that PDZ3 of whirlin binds to the C-terminal region of MPP1 ($MPP1^{E\text{-}end}$) containing the atypical PDZ binding motif (PBM). Constructs containing PDZ1+2 of whirlin did not bind (yeast two-hybrid data not shown). We could confirm binding of $whirlin^{PDZ3}$ to GST–$MPP1^{E\text{-}end}$, but not GST–$MPP1^{GUK}$ or unfused GST in a GST-pull down assay (Fig. 4C). Using homology modeling of the interaction of

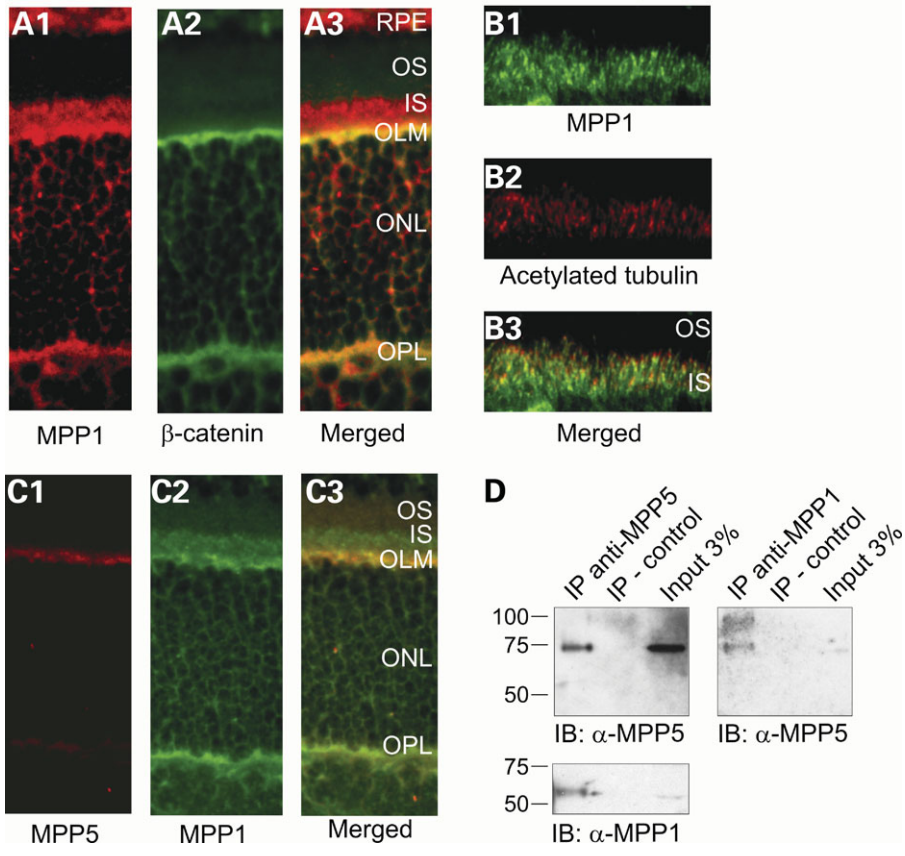

Figure 3. MPP1 and MPP5 interact at the outer limiting membrane of the neural retina. (**A**) Staining of retinal cryosections using MPP1 rabbit serum (red) detected the protein at the OPL, ONL, OLM, IS, RPE and at the connecting cilium region. (**A2**) Co-staining with an anti-β-catenin antibody (green signal), a marker for the OLM and OPL, confirmed the presence of MPP1 at these locations, as shown by the yellow signal in the overlay (**A3**). (**B**) Co-staining of MPP1 with an antibody against the connecting cilium marker acetylated tubulin. (**C1**) Anti-MPP5 only stained the OLM, and costaining with anti-MPP1 (**C2**) indicates their co-localization in the overlay (**C3**). (**D**) Immunoprecipitation with MPP5 antibody precipitates MPP5 (75 kDa) as well as MPP1 (55 kDa) from bovine retina (left panels, IP control is IgG). In the reverse experiment, MPP1 antibody co-immunoprecipitates MPP5 from mouse retina (right panel).

the PBM at the C-terminus of MPP1 with PDZ3 of whirlin, we were able to predict that this interaction is structurally feasible (Fig. 4D). Strikingly, when using a mutant MPP1 protein with a C-terminal 9 amino acid deletion in these interaction studies, binding to the long isoform of whirlin was not absent, only reduced compared with the full-length MPP1 protein. A similarly weak binding could be observed for full-length whirlin and the $MPP1^{GUK}$ fragment (Fig. 4E). These findings point to an additional interaction mechanism, besides the PDZ–PBM mechanism.

Recently, a complex of whirlin and MPP1 was described to localize to the stereocilia tips in hair cells of the inner ear (29), but a similar complex in the retina has never been reported. Excitingly, the localization of MPP1 in the retina strongly resembled the localization pattern of whirlin (26). Immunohistochemical analysis of rat retinal sections using antibodies against whirlin and MPP1 clearly confirmed the colocalization of both proteins at the OPL, the OLM, at the region of the CC and somewhat weaker at the IS (Fig. 5A and B). In order to confirm the presence of both proteins in the same retinal protein complex, we performed co-immunoprecipitation analysis. The anti-whirlin antibody efficiently precipitated whirlin (Fig. 5C, top panel), and MPP1 coprecipitated as part of the same protein complex from the mouse retina (Fig. 5C, bottom panel).

The distinct colocalization of MPP1 and whirlin at the CC is particularly interesting, as this region has been shown to harbor many proteins associated with inherited retinal degeneration. Mutations in the centrosome/ciliary protein CEP290 (NPHP6) (31,32) and the ciliary protein lebercilin (33) are causative for LCA, while mutations in motor protein Myosin VIIa are responsible for Usher syndrome type 1B (34). Aberrations in Retinitis Pigmentosa GTPase Regulator (RPGR) and its interacting protein (RPGRIP1) are causative for X-linked retinitis pigmentosa and LCA, respectively (35–39). We therefore analyzed the CC region in detail by immunoelectron microscopy (Fig. 5D and E). Using specific antibodies against whirlin and MPP1, we determined the localization of both proteins in the basal bodies and the CC itself. In addition, whirlin is detected in the calycal processes surrounding the CC.

DISCUSSION

Basic cell polarity and cell adhesion processes that are intimately connected, govern the formation and maintenance of

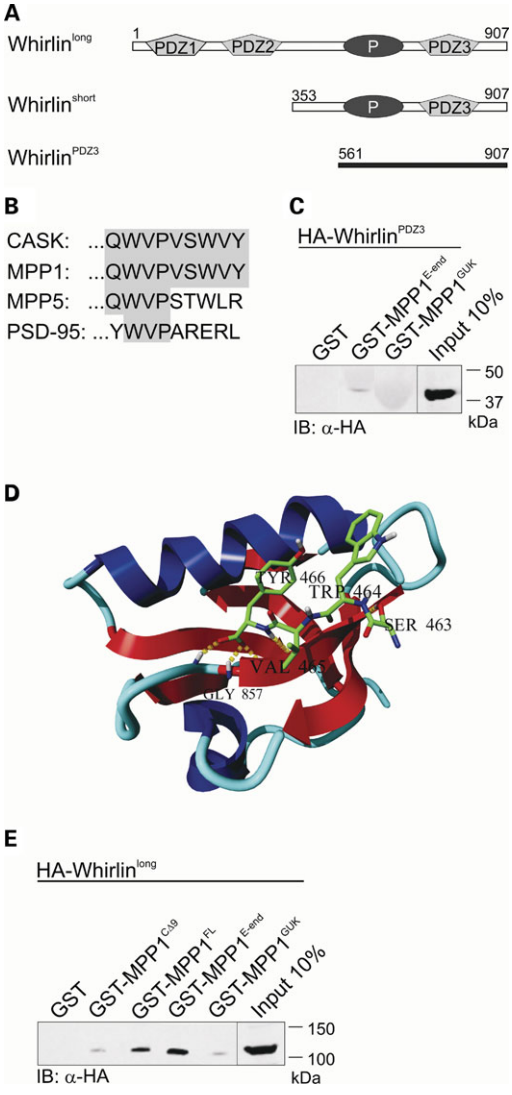

Figure 4. Whirlin can bind to MPP1 by two different mechanisms. (**A**) Schematic representation of the long and short isoform of whirlin. The short isoform has an alternative starting sequence of 37 amino acids. Starting position is indicated relative to the long isoform. Both isoforms contain a proline-rich region (P) and the PDZ3 domain. A construct that contains the PDZ3 domain of whirlin is used for further biochemical analysis. (**B**) Alignment of the nine C-terminal amino acids after the GUK domain of different MAGUK proteins. (**C**) Bacterially expressed GST-fusion proteins of $MPP1^{E\text{-}end}$ and $MPP1^{GUK}$ were used to determine the minimal binding domain required for interaction with the PDZ3 domain of HA-tagged whirlin. GST–$MPP1^{E\text{-}end}$ did bind to $whirlin^{PDZ3}$, whereas MPP1 containing only the GUK domain did not. Some background signal of GST-fusion proteins is detected in lane 2 and 3. (**D**) Homology modeling of the MPP1 C-terminus bound to the C-terminal whirlin PDZ3 domain (PDB 1UFX) indicates that the core motif of the interaction is the peptide's C-terminal carboxyl group tightly bound by three backbone NH groups, a common feature in PDZ–PBM interactions. However, this interaction is not possible in 1UFX (the whirlin PDZ structure) since one peptide plane is flipped and a C=O faces the carboxyl group. Therefore, it is predicted that Gly 857 in whirlin must undergo a conformational change to allow binding, which is represented in the figure. (**E**) The full length HA-tagged whirlin can bind to the GST-fused full-length MPP1 protein without the C-terminal nine amino acids of MPP1 (GST–$MPP1^{C\Delta 9}$). However, the interaction with $MPP1^{FL}$, the full-length protein that contains the PBM is stronger (equal amounts of proteins were used). The C-terminal part of MPP1 ($MPP1^{E\text{-}end}$) also binds strongly to full-length whirlin, whereas the GUK domain of MPP1 ($MPP1^{GUK}$) without the PBM still has reduced affinity.

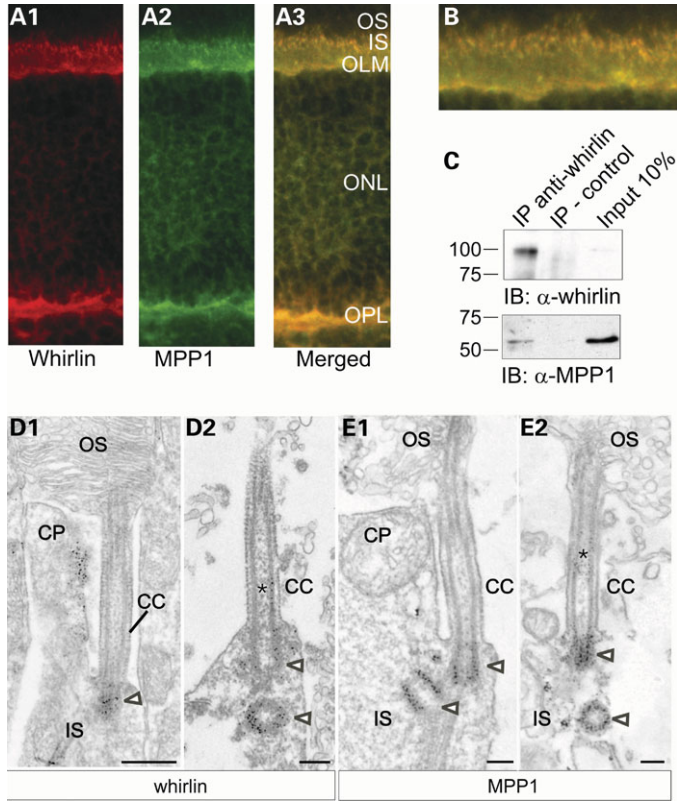

Figure 5. MPP1 interacts with whirlin in photoreceptors. (**A, B**) Retinal cryosections were stained using polyclonal antibodies against whirlin (**A1**) and MPP1 (**A2**). The signals show a near-complete overlap in the overlay (**A3**). (**B**) The most prominent staining was found at the OPL, OLM and around the inner segments (IS). (**C**) Immunoprecipitation of whirlin using a polyclonal anti-whirlin antibody precipitated whirlin from mouse retinal lysates (top). MPP1 co-precipitated with anti-whirlin (bottom). As a control, protein A/G agarose beads without primary antibody were used. (**D**) Pre-embedding immunolabeling of the ciliary region of mouse photoreceptors by antibodies against whirlin shows a clear staining of the calycal processes (CP), the basal bodies (arrow heads) (**D1** and **D2**) and of the connecting cilium (indicated by asterisks) (**D2**). Sections stained with anti-MPP1 show an identical signal in the basal bodies and the connecting cilium (**E1** and **E2**), but not in the calycal process. Bars in D1, 0.5 μm; D2, 0.25 μm; E1 and E2, 0.2 μm.

the layered structure of the retina. Although the association with polarity defects is not yet well understood, loss of the correct apico-basal distribution of the associated protein complexes at the cell membranes may trigger the developmental disorganization. In this study, we have assessed one of the key members of the apico-basal polarity complexes, MPP5, for protein–protein interactions that could provide clues for its involvement in retinal patterning. We identified MPP1 as a novel interactor, and by homology modeling predicted a binding mechanism of homo- as well as heterodimerization of the MAGUK modules. Our data indicate that this only occurs in specific orientations of these modules.

MPP1 is known to bind glycophorin C and protein 4.1 in a complex that facilitates subcortical cytoskeleton-membrane linkage in erythrocytes and has a scaffold function in post-synaptic regions of neurons in the brain (40,41). A role for this protein in the retina, however, has never been described. Our findings indicate that MPP1 has several functions in the retina. As a novel member of the Crumbs/MPP5 protein

network, it may be a crucial factor in connecting the Crumbs protein complexes and/or the actin cytoskeleton to the membrane, analogous to its function in erythrocytes. Its binding to the transmembrane protein glycophorin-C (42) and CASK (43) was not studied here, but may also be needed to provide an accurate docking point to establish specific membrane subcompartments, either in synaptic processes in the OPL or at the OLM.

We demonstrate that the *MPP1* gene is ubiquitously expressed, in adult tissues and throughout development. Its expression in the retina showed striking similarities to the retinal expression pattern of *DFNB31*, the gene encoding whirlin (26). During development of the retina, expression is highest in the inner, neuroblastic layer, while at later stages it is also present in the photoreceptor cell layer. The increasing expression of whirlin and MPP1 in the inner neuroblastic layer during early development may implicate that these proteins indeed play a role at the early stages of retinal pattern formation.

Multi-PDZ protein whirlin is associated with inherited isolated deafness (DFNB31) (27) and Usher syndrome (USH2D) (28). We and others recently identified whirlin as a key player in the Usher protein network both in the retina and in the inner ear (26,44). As the whirlin–MPP1 interaction was previously identified as a preliminary result from a yeast two-hybrid screen, but without further confirmation (30), we analyzed the direct interaction of whirlin and MPP1. We confirmed the interaction in the yeast two-hybrid system, by GST-pull down analysis and by co-immunoprecipitation from retinal extracts. We could also specify the binding mechanism to a classical PDZ-amino terminal PBM interaction, in combination with a second mechanism, which most likely involves different internal epitopes. Very recently, the MPP1–whirlin interaction was also identified in the inner ear at the stereocilia tip (29). Our PDZ3–PBM interaction data specify in more detail the PDZ3–GUK interaction that was suggested by Mburu *et al*. (29).

Interaction of MPP1 with whirlin may provide a physical connection of the Usher protein network and the Crumbs protein complex at the OLM, via MPP5. A schematic representation of these interactions is given in Figure 6. It was also previously shown, that other MPP5-associated members of the Crumbs protein complex are present at the OLM (18,19), as is true for multiple whirlin-associated members of the Usher protein network (26,45). MPP5 localization is limited to the OLM, whereas MPP1 is also present at the synaptic layer (OPL), the IS and the region of the CC, in a pattern strongly resembling the retinal localization of the Usher syndrome-associated proteins whirlin, USH2A and VLGR-1 (26). Detailed immunoelectron microscopy analysis revealed the presence of both MPP1 and whirlin in the basal bodies and, to a somewhat lesser extent, in the ciliary axoneme of the photoreceptor cilium. We also detected whirlin in the calycal processes of the photoreceptor, the periciliary region. MPP1 was not found at this specific subcellular site. The role of the whirlin–MPP1 interaction at the CC and basal bodies remains to be determined, but a number of findings suggest a role for both proteins in actin organization and dynamics. Interaction of whirlin with myosin XVa suggests a role in polymerization of the actin filaments that extend

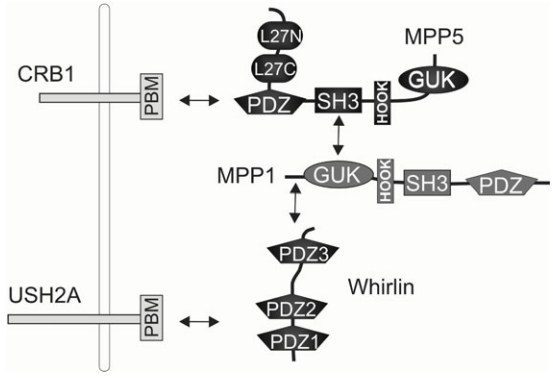

Figure 6. Schematic representation of the link between the Crumbs and Usher protein networks via MPP1. Transmembrane proteins CRB1 and Usher2A bind with their PDZ binding motifs (PBM) to the PDZ domain of MPP5 and PDZ1/PDZ2 of whirlin, respectively. MPP5 interacts with MPP1 via the SH3–GUK-domain binding mechanism, while the C-terminus of MPP1 is involved in binding to PDZ3 of whirlin. An additional binding mechanism is involved in the latter, which remains to be specified.

beneath the ciliary membrane (similar as in stereocilia development) (46,47), while association with myosin VIIa provides a link to actin-based opsin transport in the CC (48). The known association of MPP1 with 4.1R and the recently identified colocalization in stereocilia of the inner ear suggest a role in actin organization beyond their function in erythrocytes (29,49). Alternatively or simultaneously, MPP1–whirlin may also contribute to the maintenance of a radial microtubule organization at the basal bodies and CC by 4.1R, similar to the role of 4.1R in centrosomes (50).

The colocalization of MPP1, MPP5 and whirlin in the retina indicates the complementary nature of their interaction. Although the exact roles of these newly identified partnerships in the retina remain to be determined, our current findings suggest a link between the core developmental processes of actin polymerization and cell polarity establishment or maintenance through MPP1. We argue that their interaction, colocalization and coexpression patterns are in line with an important role in generating apico-basal polarity and patterning of the retina, processes that may be disrupted in the inherited disorders associated with defects in the Crumbs and Usher protein networks.

MATERIALS AND METHODS

Animals

Wistar rats (Harlan, The Netherlands) and B6/129 F1 mice used for this study were housed under normal conditions with access to food and water *ad libitum*. All animals were treated in accordance with international and institutional guidelines.

DNA constructs

Human retinal cDNA was used to clone full-length *MPP5* as well as the SH3 + HOOK domain (amino acids 337–477), HOOK-end (amino acids 408–675) as described previously (19). cDNAs encoding human full-length *whirlin* (amino acids 1–907), PDZ1 (amino acids 138–233) and PDZ2

(amino acids 279–360) were cloned in the pDONR201 vector as previously described (45). Full-length human *MPP1* was cloned using IMAGE clone no. 2820598. All *MPP1* and *whirlin* constructs were made by PCR using the GATEWAY cloning system (Invitrogen, Groningen, the Netherlands) using the full-length constructs as a template according to the manufacturer's procedures. Gene-specific primers that were used are listed in Supplementary Material, Table S2.

Yeast two-hybrid

A GAL4-based yeast two-hybrid system (Hybrizap, Stratagene) was used to screen for proteins that interact with MPP5. The DNA binding domain (pBD) fused to the SH3 and HOOK domain of MPP5 in PJ69-4A was used as bait on a human oligo-dT primed retinal cDNA library (19). The human oligo-dT primed retinal cDNA library was transformed in PJ69-4α and contained 2.1×10^6 primary clones. Positive clones were obtained by cell-to-cell mating with an efficiency of 3.4%, resulting in a total number of 13×10^6 clones on selection plates lacking tryptophan, leucine, histidine and adenine. In total, 11 clones that contained MPP1 were selected based on growth on these plates and by α- and β-galactosidase activity. To map the interacting domains of MPP5, MPP1 and whirlin, constructs fused to pAD and pBD were co-transformed in PJ694α. If yeast clones grow on selection plates and show coloring in the α- and β-galactosidase activity assays, a protein pair is indicated positive for interaction.

Antibodies

For immunostaining the following antibodies were used: anti-β-catenin (1:500, Transduction Laboratories), anti-MPP5 (SN47, 1:250, Dr J. Wijnholds) (19), anti-MPP1 mouse serum A01 (1: 300, Abnova), anti-MPP1 rabbit serum (1:300, Dr A.H. Chishti) (51), anti-whirlin raised against a GST-fusion protein encoding a fragment (amino acids 701–765) of the long isoform [1:500 (26)]. Secondary antibodies were conjugated with Alexa 488 or Alexa 568 (Molecular Probes, Leiden, the Netherlands). For immunoprecipitation the following antibodies were used: anti-MPP5 SN47, anti-MPP1N-19 (Santa-Cruz), anti-whirlin (26), mouse anti-chicken IgG clone CG-106 (Sigma). Secondary antibodies: goat anti-chicken HRP, donkey anti-goat HRP, rabbit anti-guinea pig HRP from Abcam were used.

GST-pull down and immunoprecipitations

IPTG-inducible BL21–DE3 cells were transformed with GST–MPP5$^{SH3+HOOK}$/pDest15, GST–MPP1$^{E\text{-}end}$/pDest15, GST–MPP1^{FL}/pDest15, GST–MPP1^{Cdel9}/pDest15, GST–MPP1^{GUK}/pDest15, His-MBP-MPP5$^{SH3+HOOK}$/pDest566 or His-MBP-MPP1$^{E\text{-}end}$/pDest566. Bacterial cell lysates were prepared as previously described (52). Equal amounts of blocked (1.5 mg/ml BSA) glutathione Sepharose 4B beads (Amersham Pharmacia) with GST, GST fusion proteins or beads alone were incubated with 1 ml of bacterial lysates containing His-MBP-fusion proteins overnight at 4°C. HA-tagged full length whirlin or PDZ3 of whirlin was expressed in Cos-1 cells as described previously (26). Cos-1 were lysed in 50 mM Tris pH 7.5, 150 mM NaCl, 0.5% Triton X-100 and passed several times through a needle. Equal amounts of Cos-1 cell lysate were incubated with GST–MPP1 fusion proteins overnight at 4°C. After several washes with lysis buffer and TBS containing 1% Triton X-100 and 2 mM DTT, beads were boiled and proteins were resolved on SDS–PAGE. For western blotting, proteins were electrophoretically transferred onto nitrocellulose membranes, blocked in 5% milk (BioRad) and incubated with primary rabbit antibody anti-His (H-15, Santa Cruz) or mouse monoclonal anti-HA (Sigma) and secondary antibody goat anti-rabbit Alexa680 (Molecular probes) or goat anti-mouse IRDye800 (Rockland). The bands were visualized using the Odyssey infrared imaging system (LI-COR Biosciences).

For immunoprecipitations, bovine retinas obtained from the slaughterhouse or mouse retinas (P90) were used. Cytosolic and membrane fractions were prepared as described previously (18). Mouse monoclonal anti-chicken IgGs were precoupled to Dynabeads protein G (Invitrogen, Groningen, the Netherlands, 15 μg/reaction), followed by a second round of coupling of chicken anti-MPP5 antibody SN47 (10 μg/reaction). Both antibodies were covalently cross-linked to the magnetic beads using DMP (Pierce) according to manufacturer's procedures described in the Dynabeads protocol. These beads were incubated with the bovine retinal membrane fraction for 2 h at 4°C. MPP 1N-19 antibody (10 μg/reaction) was covalently coupled to Dynabeads protein G beads and subsequently incubated with the membrane fraction of mouse retinas for 2 h at 4°C. Protein A/G agarose beads (Santa Cruz) were incubated with 2 μl of whirlin antibody, followed by overnight incubation with precleared mouse retinal cytosolic extract. After incubations, the beads were pelleted and washed three times with extraction buffer or lysis buffer for the cytosolic fraction and membrane fraction, respectively. Beads were boiled and proteins were resolved on SDS–PAGE. For western blotting, proteins were electrophoretically transferred onto nitrocellulose or PVDF membranes, blocked with 5% non-fat dry milk (Biorad) in PBST (0.1% Tween) and analyzed with the appropriate primary and HRP secondary antibodies in 1% milk in PBST. For the analysis of MPP1 in the co-immunoprecipitation experiment with MPP5, anti-MPP1 mouse serum A01 (Abnova) was used. Bands were visualized using Supersignal West Pico Chemiluminescent substrate from Pierce.

Expression profiling

Total RNA was isolated from different human tissues, a D407 cell line and an ARPE-19 cell-line as described previously (53). For the semi-quantitative RT–PCR, 3.1 μg RNA was reverse-transcribed using random hexanucleotides (54). A touchdown PCR was performed on 62 ng cDNA for the *MPP1-7* genes and the housekeeping gene *GUS*, which served as a standard. Used primer combinations are described in supporting materials and methods.

In situ hybridization

Mouse embryos (E12.5–E18.5) and adult mice (P7 and P90) were collected and prepared for *in situ* hybridization as

described previously (26). The *MPP1* probe contains the last three exons and part of the 3′-UTR.

Immunohistochemistry

Unfixed eyes of Wistar rats (P20) and mice (P90) were isolated and frozen in melting isopentane. Cryosections of 10 μm were made and treated with 0.01% Tween-20 in PBS followed by a blocking step with blocking solution (0.1% ovalbumin; 0.5% fish gelatin in PBS) as described previously (26). Sections were incubated overnight with primary antibody diluted in blocking solution and for 1 h with secondary antibody conjugated to Alexa 488 or 568 (Molecular Probes, the Netherlands). Sections were embedded with Prolong Gold Anti-fade (Molecular Probes). For imaging, a Zeiss Axioscop 2 fluorescence microscope with Axiovision software was used.

Pre-embedding immunoelectron microscopy

Labeling was performed as described previously (55). Vibratome sections through mouse retina were stained by primary antibodies against whirlin and MPP1 and visualized by appropriate secondary antibodies (Vectastain ABC-Kit, Vector, UK). After fixation with 0.5% OsO_4 specimens were embedded in araldite and ultrathin sections were analyzed with a FEI Tecnai 12 TEM.

Molecular modeling of MPP1 and MPP5

The homology model of MPP1 (Swiss Prot entry EM55_HUMAN) was built using the protocol described for MPP4 and MPP5 previously (19). The modeling template was again the SH3-GUK module of Postsynaptic Density Protein 95 (PSD-95) with approximately 40% sequence identity, solved at 1.8 Å resolution (56) (PDB ID 1KJW). To estimate the relative affinities (Table 1) of the three homodimers (MPP1-1, MPP4-4, MPP5-5) and the three heterodimers (MPP1-4, MPP1-5, MPP4-5), molecular models of all nine different SH3–GUK complexes were derived by permutating the domains of the initial models and re-optimizing the side-chains with the molecular modeling program YASARA (www.yasara.org), such that the NOVA force field energy was minimal and binding energies could be calculated (19,57,58). Coordinate files of the models are available from the authors upon request.

SUPPLEMENTARY MATERIAL

Supplementary Material is available at HMG Online.

ACKNOWLEDGEMENTS

The authors thank E. Sehn for technical assistance. Antibodies were kindly provided by Dr J. Wijnholds (anti-MPP5 SN47), and Dr A.H. Chishti (anti-MPP1 serum). This research was supported by grants from the Netherlands Organization for Scientific Research [NWO; grant 912-02-018 (to F.P.M.C)], the Algemene Nederlandse Vereniging ter Voorkoming van Blindheid (to R.R. and F.P.M.C), BRPS project GR552 (to H.K. and R.R), EVI-GENORET [LSHG-CT-2005 512036 (to R.R. and F.P.M.C.)], DFG [GRK 1044 (to U.W.)], the FAUN-Stiftung (to U.W.) and the FcB-Initiative Usher Syndrome (to U.W. and H.K.).

Conflict of Interest statement. There are no conflicts of interest.

REFERENCES

1. Malicki, J. (2004) Cell fate decisions and patterning in the vertebrate retina: the importance of timing, asymmetry, polarity and waves. *Curr. Opin. Neurobiol.*, **14**, 15–21.
2. Wei, X. and Malicki, J. (2002) nagie oko, encoding a MAGUK-family protein, is essential for cellular patterning of the retina. *Nat. Genet.*, **31**, 150–157.
3. Malicki, J., Neuhauss, S.C., Schier, A.F., Solnica-Krezel, L., Stemple, D.L., Stainier, D.Y., Abdelilah, S., Zwartkruis, F., Rangini, Z. and Driever, W. (1996) Mutations affecting development of the zebrafish retina. *Development*, **123**, 263–273.
4. Malicki, J. and Driever, W. (1999) oko meduzy mutations affect neuronal patterning in the zebrafish retina and reveal cell–cell interactions of the retinal neuroepithelial sheet. *Development*, **126**, 1235–1246.
5. Pujic, Z. and Malicki, J. (2001) Mutation of the zebrafish glass onion locus causes early cell-nonautonomous loss of neuroepithelial integrity followed by severe neuronal patterning defects in the retina. *Dev. Biol.*, **234**, 454–469.
6. Jensen, A.M., Walker, C. and Westerfield, M. (2001) mosaic eyes: a zebrafish gene required in pigmented epithelium for apical localization of retinal cell division and lamination. *Development*, **128**, 95–105.
7. Wei, X., Zou, J., Takechi, M., Kawamura, S. and Li, L. (2006) Nok plays an essential role in maintaining the integrity of the outer nuclear layer in the zebrafish retina. *Exp. Eye Res.*, **83**, 31–44.
8. Omori, Y. and Malicki, J. (2006) oko meduzy and related crumbs genes are determinants of apical cell features in the vertebrate embryo. *Curr. Biol.*, **16**, 945–957.
9. Horne-Badovinac, S., Lin, D., Waldron, S., Schwarz, M., Mbamalu, G., Pawson, T., Jan, Y., Stainier, D.Y. and Abdelilah-Seyfried, S. (2001) Positional cloning of heart and soul reveals multiple roles for PKC lambda in zebrafish organogenesis. *Curr. Biol.*, **11**, 1492–1502.
10. Malicki, J., Jo, H. and Pujic, Z. (2003) Zebrafish N-cadherin, encoded by the glass onion locus, plays an essential role in retinal patterning. *Dev. Biol.*, **259**, 95–108.
11. Jensen, A.M. and Westerfield, M. (2004) Zebrafish mosaic eyes is a novel FERM protein required for retinal lamination and retinal pigmented epithelial tight junction formation. *Curr. Biol.*, **14**, 711–717.
12. Laprise, P., Beronja, S., Silva-Gagliardi, N.F., Pellikka, M., Jensen, A.M., McGlade, C.J. and Tepass, U. (2006) The FERM protein Yurt is a negative regulatory component of the Crumbs complex that controls epithelial polarity and apical membrane size. *Dev. Cell*, **11**, 363–374.
13. Knust, E. and Bossinger, O. (2002) Composition and formation of intercellular junctions in epithelial cells. *Science*, **298**, 1955–1959.
14. Bachmann, A., Schneider, M., Theilenberg, E., Grawe, F. and Knust, E. (2001) *Drosophila* Stardust is a partner of Crumbs in the control of epithelial cell polarity. *Nature*, **414**, 638–643.
15. Hong, Y., Stronach, B., Perrimon, N., Jan, L.Y. and Jan, Y.N. (2001) *Drosophila* Stardust interacts with Crumbs to control polarity of epithelia but not neuroblasts. *Nature*, **414**, 634–638.
16. Richard, M., Roepman, R., Aartsen, W.M., van Rossum, A.G., den Hollander, A.I., Knust, E., Wijnholds, J. and Cremers, F.P.M. (2006) Towards understanding CRUMBS function in retinal dystrophies. *Hum. Mol. Genet.*, **15**(Spec no. 2), R235–R243.
17. Mehalow, A.K., Kameya, S., Smith, R.S., Hawes, N.L., Denegre, J.M., Young, J.A., Bechtold, L., Haider, N.B., Tepass, U., Heckenlively, J.R. *et al.* (2003) CRB1 is essential for external limiting membrane integrity and photoreceptor morphogenesis in the mammalian retina. *Hum. Mol. Genet.*, **12**, 2179–2189.
18. van de Pavert, S.A., Kantardzhieva, A., Malysheva, A., Meuleman, J., Versteeg, I., Levelt, C., Klooster, J., Geiger, S., Seeliger, M.W., Rashbass, P. *et al.* (2004) Crumbs homologue 1 is required for

maintenance of photoreceptor cell polarization and adhesion during light exposure. *J. Cell Sci.*, **117**, 4169–4177.
19. Kantardzhieva, A., Gosens, I., Alexeeva, S., Punte, I.M., Versteeg, I., Krieger, E., Neefjes-Mol, C.A., den Hollander, A.I., Letteboer, S.J., Klooster, J. *et al.* (2005) MPP5 recruits MPP4 to the CRB1 complex in photoreceptors. *Invest. Ophthalmol. Vis. Sci.*, **46**, 2192–2201.
20. Kantardzhieva, A., Alexeeva, S., Versteeg, I. and Wijnholds, J. (2006) MPP3 is recruited to the MPP5 protein scaffold at the retinal outer limiting membrane. *FEBS J.*, **273**, 1152–1165.
21. Kamberov, E., Makarova, O., Roh, M., Liu, A., Karnak, D., Straight, S. and Margolis, B. (2000) Molecular cloning and characterization of Pals, proteins associated with mLin-7. *J. Biol. Chem.*, **275**, 11425–11431.
22. Hurd, T.W., Gao, L., Roh, M.H., Macara, I.G. and Margolis, B. (2003) Direct interaction of two polarity complexes implicated in epithelial tight junction assembly. *Nat. Cell Biol.*, **5**, 137–142.
23. Roh, M.H., Makarova, O., Liu, C.J., Shin, K., Lee, S., Laurinec, S., Goyal, M., Wiggins, R. and Margolis, B. (2002) The Maguk protein, Pals1, functions as an adapter, linking mammalian homologues of Crumbs and Discs Lost. *J. Cell Biol.*, **157**, 161–172.
24. Cao, X., Ding, X., Guo, Z., Zhou, R., Wang, F., Long, F., Wu, F., Bi, F., Wang, Q., Fan, D. *et al.* (2005) PALS1 specifies the localization of ezrin to the apical membrane of gastric parietal cells. *J. Biol. Chem.*, **280**, 13584–13592.
25. McHugh, E.M., Zhu, W., Milgram, S. and Mager, S. (2004) The GABA transporter GAT1 and the MAGUK protein Pals1: interaction, uptake modulation, and coexpression in the brain. *Mol. Cell Neurosci.*, **26**, 406–417.
26. van Wijk, E., van der Zwaag, B., Peters, T., Zimmermann, U., Te Brinke, H., Kersten, F.F.J., Marker, T., Aller, E., Hoefsloot, L.H., Cremers, C.W.R.J. *et al.* (2006) The DFNB31 gene product whirlin connects to the Usher protein network in the cochlea and retina by direct association with USH2A and VLGR1. *Hum. Mol. Genet.*, **15**, 751–765.
27. Mburu, P., Mustapha, M., Varela, A., Weil, D., El Amraoui, A., Holme, R.H., Rump, A., Hardisty, R.E., Blanchard, S., Coimbra, R.S. *et al.* (2003) Defects in whirlin, a PDZ domain molecule involved in stereocilia elongation, cause deafness in the whirler mouse and families with DFNB31. *Nat. Genet.*, **34**, 421–428.
28. Ebermann, I., Scholl, H.P., Charbel, I.P., Becirovic, E., Lamprecht, J., Jurklies, B., Millan, J.M., Aller, E., Mitter, D. and Bolz, H. (2006) A novel gene for Usher syndrome type 2: mutations in the long isoform of whirlin are associated with retinitis pigmentosa and sensorineural hearing loss. *Hum. Genet*., **121**, 203–211.
29. Mburu, P., Kikkawa, Y., Townsend, S., Romero, R., Yonekawa, H. and Brown, S.D. (2006) Whirlin complexes with p55 at the stereocilia tip during hair cell development. *Proc. Natl Acad. Sci. USA*, **103**, 10973–10978.
30. Yap, C.C., Liang, F., Yamazaki, Y., Muto, Y., Kishida, H., Hayashida, T., Hashikawa, T. and Yano, R. (2003) CIP98, a novel PDZ domain protein, is expressed in the central nervous system and interacts with calmodulin-dependent serine kinase. *J. Neurochem.*, **85**, 123–134.
31. Chang, B., Khanna, H., Hawes, N., Jimeno, D., He, S., Lillo, C., Parapuram, S.K., Cheng, H., Scott, A., Hurd, R.E. *et al.* (2006) In-frame deletion in a novel centrosomal/ciliary protein CEP290/NPHP6 perturbs its interaction with RPGR and results in early-onset retinal degeneration in the rd16 mouse. *Hum. Mol. Genet.*, **15**, 1847–1857.
32. den Hollander, A.I., Koenekoop, R.K., Yzer, S., Lopez, I., Arends, M.L., Voesenek, K.E., Zonneveld, M.N., Strom, T.M., Meitinger, T., Brunner, H.G. *et al.* (2006) Mutations in the CEP290 (NPHP6) gene are a frequent cause of Leber congenital amaurosis. *Am. J. Hum. Genet.*, **79**, 556–561.
33. den Hollander, A.I., Koenekoop, R.K., Mohamed, M.D., Arts, H.H., Boldt, K., Towns, K.V., Sedmak, T., Beer, M., Nagel-Wolfrum, K., McKibbin, M. *et al.* (2007) Mutations in LCA5, encoding the ciliary protein lebercilin, cause Leber congenital amaurosis. *Nat. Genet.*, doi:10.1038/ng2066.
34. Weil, D., Levy, G., Sahly, I., Levi-Acobas, F., Blanchard, S., El Amraoui, A., Crozet, F., Philippe, H., Abitbol, M. and Petit, C. (1996) Human myosin VIIA responsible for the Usher 1B syndrome: a predicted membrane-associated motor protein expressed in developing sensory epithelia. *Proc. Natl Acad. Sci. USA*, **93**, 3232–3237.
35. Hong, D.H., Yue, G., Adamian, M. and Li, T. (2001) Retinitis pigmentosa GTPase regulator (RPGRr)-interacting protein is stably associated with the photoreceptor ciliary axoneme and anchors RPGR to the connecting cilium. *J. Biol. Chem.*, **276**, 12091–12099.
36. Hong, D.H., Pawlyk, B., Sokolov, M., Strissel, K.J., Yang, J., Tulloch, B., Wright, A.F., Arshavsky, V.Y. and Li, T. (2003) RPGR isoforms in photoreceptor connecting cilia and the transitional zone of motile cilia. *Invest. Ophthalmol. Vis. Sci.*, **44**, 2413–2421.
37. Meindl, A., Dry, K., Herrmann, K., Manson, F., Ciccodicola, A., Edgar, A., Carvalho, M.R., Achatz, H., Hellebrand, H., Lennon, A. *et al.* (1996) A gene (RPGR) with homology to the RCC1 guanine nucleotide exchange factor is mutated in X-linked retinitis pigmentosa (RP3). *Nat. Genet*, **13**, 35–42.
38. Roepman, R., van Duynhoven, G., Rosenberg, T., Pinckers, A.J.L.G., Bleeker-Wagemakers, E.M., Bergen, A.A.B., Post, J., Beck, A., Reinhardt, R., Ropers, H.-H. *et al.* (1996) Positional cloning of the gene for X-linked retinitis pigmentosa: homology with the guanine-nucleotide-exchange factor RCC1. *Hum. Mol. Genet.*, **5**, 1035–1041.
39. Koenekoop, R.K. (2005) RPGRIP1 is mutated in Leber congenital amaurosis: a mini-review. *Ophthalmic Genet.*, **26**, 175–179.
40. Chishti, A.H. (1998) Function of p55 and its nonerythroid homologues. *Curr. Opin. Hematol.*, **5**, 116–121.
41. Jing-Ping, Z., Tian, Q.B., Sakagami, H., Kondo, H., Endo, S. and Suzuki, T. (2005) p55 protein is a member of PSD scaffold proteins in the rat brain and interacts with various PSD proteins. *Brain Res. Mol. Brain Res.*, **135**, 204–216.
42. Marfatia, S.M., Morais-Cabral, J.H., Kim, A.C., Byron, O. and Chishti, A.H. (1997) The PDZ domain of human erythrocyte p55 mediates its binding to the cytoplasmic carboxyl terminus of glycophorin C. Analysis of the binding interface by *in vitro* mutagenesis. *J. Biol. Chem.*, **272**, 24191–24197.
43. Nix, S.L., Chishti, A.H., Anderson, J.M. and Walther, Z. (2000) hCASK and hDlg associate in epithelia, and their src homology 3 and guanylate kinase domains participate in both intramolecular and intermolecular interactions. *J. Biol. Chem.*, **275**, 41192–41200.
44. Adato, A., Lefevre, G., Delprat, B., Michel, V., Michalski, N., Chardenoux, S., Weil, D., El Amraoui, A. and Petit, C. (2005) Usherin, the defective protein in Usher syndrome type IIA, is likely to be a component of interstereocilia ankle links in the inner ear sensory cells. *Hum. Mol. Genet.*, **14**, 3921–3932.
45. Reiners, J., van Wijk, E., Marker, T., Zimmermann, U., Jurgens, K., Te Brinke, H., Overlack, N., Roepman, R., Knipper, M., Kremer, H. and Wolfrum, U. (2005) Scaffold protein harmonin (USH1C) provides molecular links between Usher syndrome type 1 and type 2. *Hum. Mol. Genet.*, **14**, 3933–3943.
46. Delprat, B., Michel, V., Goodyear, R., Yamasaki, Y., Michalski, N., El Amraoui, A., Perfettini, I., Legrain, P., Richardson, G., Hardelin, J.P. and Petit, C. (2005) Myosin XVa and whirlin, two deafness gene products required for hair bundle growth, are located at the stereocilia tips and interact directly. *Hum. Mol. Genet.*, **14**, 401–410.
47. Belyantseva, I.A., Boger, E.T., Naz, S., Frolenkov, G.I., Sellers, J.R., Ahmed, Z.M., Griffith, A.J. and Friedman, T.B. (2005) Myosin-XVa is required for tip localization of whirlin and differential elongation of hair-cell stereocilia. *Nat. Cell Biol.*, **7**, 148–156.
48. Wolfrum, U. and Schmitt, A. (2000) Rhodopsin transport in the membrane of the connecting cilium of mammalian photoreceptor cells. *Cell Motil. Cytoskeleton*, **46**, 95–107.
49. Nunomura, W., Takakuwa, Y., Parra, M., Conboy, J. and Mohandas, N. (2000) Regulation of protein 4.1R, p55, and glycophorin C ternary complex in human erythrocyte membrane. *J. Biol. Chem.*, **275**, 24540–24546.
50. Perez-Ferreiro, C.M., Vernos, I. and Correas, I. (2004) Protein 4.1R regulates interphase microtubule organization at the centrosome. *J. Cell Sci.*, **117**, 6197–6206.
51. Marfatia, S.M., Lue, R.A., Branton, D. and Chishti, A.H. (1994) *In vitro* binding studies suggest a membrane-associated complex between erythroid p55, protein 4.1, and glycophorin C. *J. Biol. Chem.*, **269**, 8631–8634.
52. Frangioni, J.V. and Neel, B.G. (1993) Solubilization and purification of enzymatically active glutathione S-transferase (pGEX) fusion proteins. *Anal. Biochem.*, **210**, 179–187.

53. Dunn, K.C., Aotaki-Keen, A.E., Putkey, F.R. and Hjelmeland, L.M. (1995) ARPE-19, a human retinal pigment epithelial cell line with differentiated properties. *Invest. Ophthalmol. Vis. Sci.*, **36**, S766.
54. den Hollander, A.I., van Driel, M.A., de Kok, Y.J.M., van de Pol, T.J.R., Hoyng, C.B., Brunner, H.G., Deutman, A.F. and Cremers, F.P.M. (1999) Isolation and mapping of novel candidate genes for retinal disorders using suppression subtractive hybridization. *Genomics*, **58**, 240–249.
55. Brandstatter, J.H., Lohrke, S., Morgans, C.W. and Wassle, H. (1996) Distributions of two homologous synaptic vesicle proteins, synaptoporin and synaptophysin, in the mammalian retina. *J. Comp. Neurol.*, **370**, 1–10.
56. McGee, A.W., Dakoji, S.R., Olsen, O., Bredt, D.S., Lim, W.A. and Prehoda, K.E. (2001) Structure of the SH3-guanylate kinase module from PSD-95 suggests a mechanism for regulated assembly of MAGUK scaffolding proteins. *Mol. Cell*, **8**, 1291–1301.
57. Krieger, E., Koraimann, G. and Vriend, G. (2002) Increasing the precision of comparative models with YASARA NOVA–a self-parameterizing force field. *Proteins*, **47**, 393–402.
58. Krieger, E., Geretti, E., Brandner, B., Goger, B., Wells, T.N. and Kungl, A.J. (2004) A structural and dynamic model for the interaction of interleukin-8 and glycosaminoglycans: support from isothermal fluorescence titrations. *Proteins*, **54**, 768–775.